Active Nematics at Bifurcations

Zhengyang Liu,[1] Claire Doré,[1] Antonio Tavera-Vazquez,[1, 2] and Teresa Lopez-Leon[1]

[1]*Laboratoire Gulliver, UMR 7083 CNRS, ESPCI Paris, PSL Research University, 75005 Paris, France.*

[2]*Pritzker School of Molecular Engineering, University of Chicago, Chicago, IL 60637, USA.*

(Dated: October 9, 2024)

Under lateral confinement, active matter self-organize into coherent flows. Such behavior implies the possibility of achieving logical operations in properly designed channel networks. Bifurcations are a key ingredient in channel networks. Understanding active matter behavior at bifurcations is therefore an important step towards a proper channel network design. In this paper, we experimentally explore active matter behavior at bifurcations using the microtubule-kinesin model system. Specifically, we compare the effects of channel length, ratchets and turning angles. Our results suggest that ratchets and turning angles help establish unambiguous polarized flow states. In contrast, channel length is a less relevant factor, which results in more frequently changing flow states. Our experiment is the first step to understanding active nematic flows in complex channel networks. The result lays the foundation for active matter logic and computation.

I. INTRODUCTION

Active matter flows spontaneously under channel confinement, forming coherent flows [1–5]. Such behavior implies several possibile applications of active matter, including serving as micro-scale transport, soft robotics and active matter logic [6, 7]. Boundary-mediated control has been shown effective in manipulating active matter in both experiments [1–4, 8–10] and simulations [11–14]. As of now, most studies have focused on the behavior of active matter in stand-alone smooth channels, which showed that active flows were intrinsically bistable [2, 3]. However, to realize the full potential of active matter channel flows, it is necessary to study the behavior of active matter in channel networks and with asymmertic geometries, as suggested in the pioneering active matter logic work by Woodhouse and Dunkel [7]. Very recently, channel networks attract more attention, and frustrated flow states have been investigated in coupled annular rings [5] and large honeycomb-like networks [15]. The other essential component of active matter logic is the diode channel, which only permits flow in one direction. While a few early works have hinted or employed asymmetric geometries, such as a kink or an array of ratchet teeth, to steer active matter flows [2, 5, 14, 16–18], a systematic study of asymmetric channels in the context of channel networks is still missing.

In this work, we filled this gap by experimentally studying the flow behavior of active matter at channel networks consisting of asymmetric channels. To obtain a clear understanding, we studied the simplest possible form of a channel network – the bifurcation – where a channel splits into two at a node. Despite of being simple, the bifurcation is a key element of more complex channel networks, and a great system to study frustrated flow states.

We use microtubule-kinesin system as the model active matter to experimentally test the behavior of active matter at bifurcations. We then introduce additional control elements, namely ratchet and angle, in an attempt to realize the diode channel envisioned in the theoretical framework, and to further steer the flow in the desired direction. Finally, we come up with a set of laws that govern the flow behavior at bifurcations, which can be used to design more complex channel networks. Our experiment is the first step to study active matter behavior in complex channel networks. It not only provides a playground to test and improve existing theories, and thus deepen our understanding of active matter behavior in complex environment, but also lays the foundation for potential applications of active flow networks in mass transport and flow computation.

II. EXPERIMENT

We use the microtubule-kinesin mixture as the model active matter system. The microtubule-kinesin system is a well-established model system for active nematics [5, 19–21]. Active nematics are typically prepared at water-oil interface, as illustrated in Fig. 1(a). The “grid” of channels are printed using a high resolution 3D printer (Nanoscribe Photonic Professional GT2). Figure 1(b) shows the design of a typical bifurcation channels. The bottom layer of the printed structure is a Y-shape channel, while the top layer is a set of “bridges” that hold the structure together. The middle layer is a set of spacers that separate the top and bottom layers, which keeps the bridges at a safe distance from the active nematics system. Figure 1(c) shows a top view of the bifurcation channels. All the three channels are of the same width $w = 100\,\mu$m, while the length of the channels are $l = 1000\,\mu$m. An unperturbed active nematics system is shown in Fig. 1(d), while the same system with the bifurcation channels set in is shown in Fig. 1(e).

The active nematics system is observed using a confocal microscope (Nikon), and images are taken at 2 Hz using a 10X objective lens. In a typical image, the field of view covers a part of all the bifurcation channels. Then, 400 µm of each channel is cropped and analyzed by PIV, as shown in Fig. 2(a).

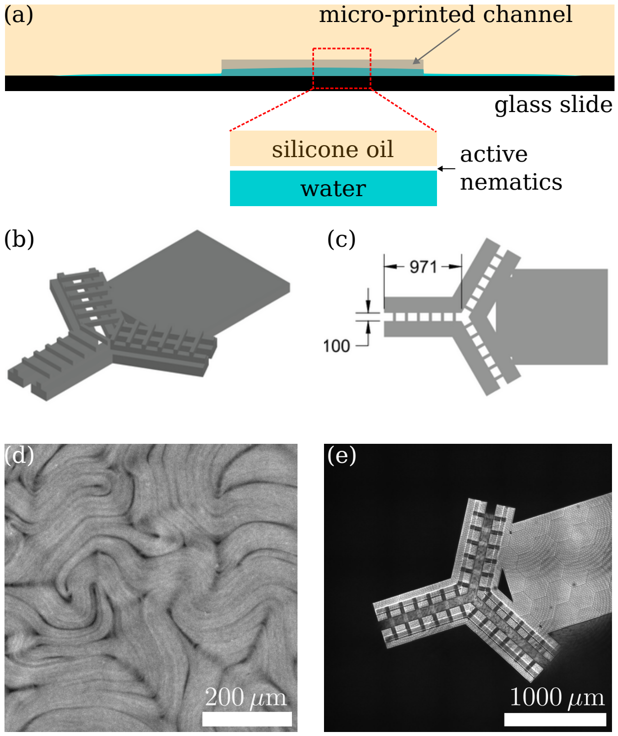

FIG. 1. **Confining microtubule-kinesin system at water-oil inerface – the experimental setup.** (a) A schematic diagram of the experimental setup. The microtubule-kinesin active nematic system is condensed at the water-oil interface, and is subject to lateral confinement by nano-printed channels. (b) A schematic diagram of the bifurcation channels. The Y-shape channel pattern is printed at the bottom. The "bridges" on the top are designed to hold the structure together. (c) Top view of the bifurcation channels. The relevant dimensions channel length l = 1000 μm and channel width w = 100 μm are labeled in place. (d) A confocal image of a mature interfacial microtubule-kinesin system. (e) A confocal image of the bifurcation channels set on the interfacial microtubule-kinesin system.

III. RESULTS

A. Symmetric bifurcation

We first study the flow behavior at a symmetric bifurcation, where all the channels are of the same length. The flow rates in the channels are plotted in Fig.2(b). The blue, orange and green curves represent the flow rates in channels A, B and C, respectively, corresponding to the colors of the borders in Fig.2(a). The light and thin curves in the back are the real flow rates, while the strong and thick curves in the front are Gaussian-smoothed flow rates with $\sigma = 25$ s. The gray curve is the sum of the flow rates in the 3 channels, which is used to verify the continuity at the junction. Due to the variation of active nematics activity, the flow rates fluctuates in time. To normalize the flow rates of different magnitudes, we define a normalizer as the maximum of the smoothed absoluted flow rates in A, B and C, as indicated by the red curve. By dividing the flow rates by the normalizer, we obtain the normalized flow rates, which are used to construct the flow rate histogram. In Fig.2(c), we show the histogram of the normalized flow rates. Instead of having a few sharp peaks, which was expected from the theoretical model [7], the histogram shows a broad and even distribution of flow rates, covering most of the possible configurations of flow rates in the 3 channels for $\phi_A < 0$. Although the channels are designed to be fully symmetric, the grid requires a base structure to which the micromanipulator is attached, which may introduce some asymmetry in the flow rates. Note that the flow rates in the 3 channels satisfy $\phi_A + \phi_B + \phi_C = 0$, so the histograms are not independent. Therefore, in the following figures, we only show the ϕ_B-ϕ_C histogram.

B. Straight channel length

Having learned from the fully symmetric bifurcation experiment, we enforce channel A as a ratchet channel, which guarantees that $\phi_A < 0$. We then study the effect of channel length on the flow behavior. In Fig.3(a), we show the flow behavior at a 9-teeth ratchet inlet with 2 equal length outlets. The flow fluctuates between polarized and non-polarized states, exploring all the possible configurations. The equal splitting state is the most probable configuration. It is also noticed that channels B and C are always outlets when fixing A as the inlet with ratchets. This observation implies that the ratchet channel has a dominant effect on the flow behavior, compared to the straight channels. Such dominance will be further confirmed in the following experiments. In Fig.3(b), we show the flow behavior at a 4-teeth ratchet inlet with long and short outlets. The expectation from theory is that the flow will prefer the longer outlet, as the longer path has a lower energy state and is therefore more energetically favorable. However, we observe that the flow explores all the possible configurations, showing no preferred splitting ratio. In Fig.3(c), we show the flow behavior at a 4-teeth ratchet inlet with 2 equal length outlets. This experiment is done to keep consistent ratchet numbers in the inlet to avoid the potential effect of ratchet number on the flow behavior. The resulting flow configuration is very similar to the longer ratchet inlet one though: the flow fluctuates between polarized and non-polarized states, exploring all the possible configurations.

C. Ratchet inlet and outlets

We then study the flow configurations of active nematics in bifurcation channels with ratchet inlets and outlets. The experimental results are shown in Fig.4. A general observation is that the peaks in the histograms are sharp, indicating that the flow configurations are more deterministic than in straight channels. When the outlet channels have different numbers of ratchet, as shown in Fig. 4(a) the flow robustly splits into different fractions in the two outlet channels. Interestingly, the flow rate ratio in the two outlet channels is almost equal to the ratio between the number of ratchet teeth. Does this unequal splitting of flow arise from the difference in the length of the channels? To answer this question, we keep the channels lengths unchanged, but modify the number of ratchet teeth in channel B, so that channels B and C has the same number of ratchet teeth. In this case, the flow robustly split into the two outlet channels with a 1:1 ratio, as shown in Fig.4(b). This result suggests that the ratchet teeth in the outlet channels play a dominant role in determining the flow behavior at bifurcations. In Fig.4(c), we show the flow behavior in channels with equal length and number of ratchet teeth. The flow again splits with a 1:1 ratio, confirming the dominant role of ratchet teeth.

[1] H Wioland, E Lushi, and R E Goldstein. Directed collective motion of bacteria under channel confinement. *New Journal of Physics*, 18(7):075002, July 2016. ISSN 1367-2630. doi:10.1088/1367-2630/18/7/075002.

[2] Kun-Ta Wu, Jean Bernard Hishamunda, Daniel T. N. Chen, Stephen J. DeCamp, Ya-Wen Chang, Alberto Fernández-Nieves, Seth Fraden, and Zvonimir Dogic. Transition from turbulent to coherent flows in confined three-dimensional active fluids. *Science*, 355(6331): eaal1979, March 2017. ISSN 0036-8075, 1095-9203. doi: 10.1126/science.aal1979.

[3] Alexandre Morin and Denis Bartolo. Flowing Active Liquids in a Pipe: Hysteretic Response of Polar Flocks to External Fields. *Physical Review X*, 8(2):021037, May 2018. doi:10.1103/PhysRevX.8.021037.

[4] Jérôme Hardoüin, Rian Hughes, Amin Doostmohammadi, Justine Laurent, Teresa Lopez-Leon, Julia M. Yeomans, Jordi Ignés-Mullol, and Francesc Sagués. Reconfigurable flows and defect landscape of confined active nematics. *Communications Physics*, 2(1):121, December 2019. ISSN 2399-3650. doi:10.1038/s42005-019-0221-x.

[5] Jérôme Hardoüin, Justine Laurent, Teresa Lopez-Leon, Jordi Ignés-Mullol, and Francesc Sagués. Active microfluidic transport in two-dimensional handlebodies. *Soft Matter*, 16(40):9230–9241, 2020. ISSN 1744-683X, 1744-6848. doi:10.1039/D0SM00610F.

[6] Sumesh P. Thampi. Channel confined active nematics. *Current Opinion in Colloid & Interface Science*, 61:101613, October 2022. ISSN 1359-0294. doi:10.1016/j.cocis.2022.101613. URL `https://www.sciencedirect.com/science/article/pii/S1359029422000528`.

[7] Francis G. Woodhouse and Jörn Dunkel. Active matter logic for autonomous microfluidics. *Nature Communications*, 8(1):15169, April 2017. ISSN 2041-1723. doi: 10.1038/ncomms15169.

[8] Enkeleida Lushi, Hugo Wioland, and Raymond E. Goldstein. Fluid flows created by swimming bacteria drive self-organization in confined suspensions. *Proceedings of the National Academy of Sciences*, 111(27):9733–9738, July 2014. ISSN 0027-8424, 1091-6490. doi: 10.1073/pnas.1405698111.

[9] Zhengyang Liu, Kechun Zhang, and Xiang Cheng. Rheology of bacterial suspensions under confinement. *Rheologica Acta*, 58(8):439–451, August 2019. ISSN 0035-4511, 1435-1528. doi:10.1007/s00397-019-01155-x.

[10] Tyler D. Ross, Heun Jin Lee, Zijie Qu, Rachel A. Banks, Rob Phillips, and Matt Thomson. Controlling organization and forces in active matter through optically defined boundaries. *Nature*, 572(7768):224–229, August 2019. ISSN 0028-0836, 1476-4687. doi:10.1038/s41586-019-1447-1.

[11] R Voituriez, J. F Joanny, and J Prost. Spontaneous flow transition in active polar gels. *Europhysics Letters (EPL)*, 70(3):404–410, May 2005. ISSN 0295-5075, 1286-4854. doi:10.1209/epl/i2004-10501-2.

[12] Davide Marenduzzo. Hydrodynamics and Rheology of Active Liquid Crystals: A Numerical Investigation. 98: 118102, 2007. doi:10.1103/PhysRevLett.98.118102.

[13] Tyler N. Shendruk, Amin Doostmohammadi, Kristian Thijssen, and Julia M. Yeomans. Dancing disclinations in confined active nematics. *Soft Matter*, 13(21):3853–3862, May 2017. ISSN 1744-6848. doi:10.1039/C6SM02310J.

[14] Jaideep P. Vaidya, Tyler N. Shendruk, and Sumesh P. Thampi. Active nematics in corrugated channels. *Soft Matter*, September 2024. ISSN 1744-6848. doi: 10.1039/D4SM00760C. URL `https://pubs.rsc.org/en/content/articlelanding/2024/sm/d4sm00760c`. Publisher: The Royal Society of Chemistry.

[15] Camille Jorge, Amélie Chardac, Alexis Poncet, and Denis Bartolo. Active hydraulics laws from frustration principles. *Nature Physics*, 20(2):303–309, February 2024. ISSN 1745-2481. doi:10.1038/s41567-023-02301-2. URL `https://www.nature.com/articles/s41567-023-02301-2`. Publisher: Nature Publishing Group.

[16] S. Elizabeth Hulme, Willow R. DiLuzio, Sergey S. Shevkoplyas, Linda Turner, Michael Mayer, Howard C. Berg, and George M. Whitesides. Using ratchets and sorters to fractionate motile cells of Escherichia coli by length. *Lab on a Chip*, 8(11):1888, 2008. ISSN 1473-0197, 1473-0189. doi:10.1039/b809892a. URL `https://xlink.rsc.org/?DOI=b809892a`.

[17] R. Di Leonardo, L. Angelani, D. Dell'Arciprete, G. Ruocco, V. Iebba, S. Schippa, M. P. Conte, F. Mecarini, F. De Angelis, and E. Di Fabrizio. Bacterial ratchet motors. *Proceedings of the National Academy of Sciences*, 107(21):9541–9545, May 2010. ISSN 0027-8424, 1091-6490. doi:10.1073/pnas.0910426107.

[18] Sattvic Ray, Jie Zhang, and Zvonimir Dogic. Rectified Rotational Dynamics of Mobile Inclusions in Two-Dimensional Active Nematics. *Physical Review Letters*, 130(23):238301, June 2023. ISSN 0031-9007, 1079-7114. doi:10.1103/PhysRevLett.130.238301. URL `https://link.aps.org/doi/10.1103/PhysRevLett.130.238301`.

[19] Tim Sanchez, Daniel T. N. Chen, Stephen J. DeCamp, Michael Heymann, and Zvonimir Dogic. Spontaneous motion in hierarchically assembled active matter. *Nature*, 491(7424):431–434, November 2012. ISSN 0028-0836, 1476-4687. doi:10.1038/nature11591.

[20] Felix C. Keber, Etienne Loiseau, Tim Sanchez, Stephen J. DeCamp, Luca Giomi, Mark J. Bowick, M. Cristina Marchetti, Zvonimir Dogic, and Andreas R. Bausch. Topology and dynamics of active nematic vesicles. *Science*, 345(6201):1135–1139, September 2014. ISSN 1095-9203. doi:10.1126/science.1254784. URL `http://dx.doi.org/10.1126/science.1254784`.

[21] Stephen J. DeCamp, Gabriel S. Redner, Aparna Baskaran, Michael F. Hagan, and Zvonimir Dogic. Orientational order of motile defects in active nematics. *Nature Materials*, 14(11):1110–1115, November 2015. ISSN 1476-1122, 1476-4660. doi:10.1038/nmat4387.

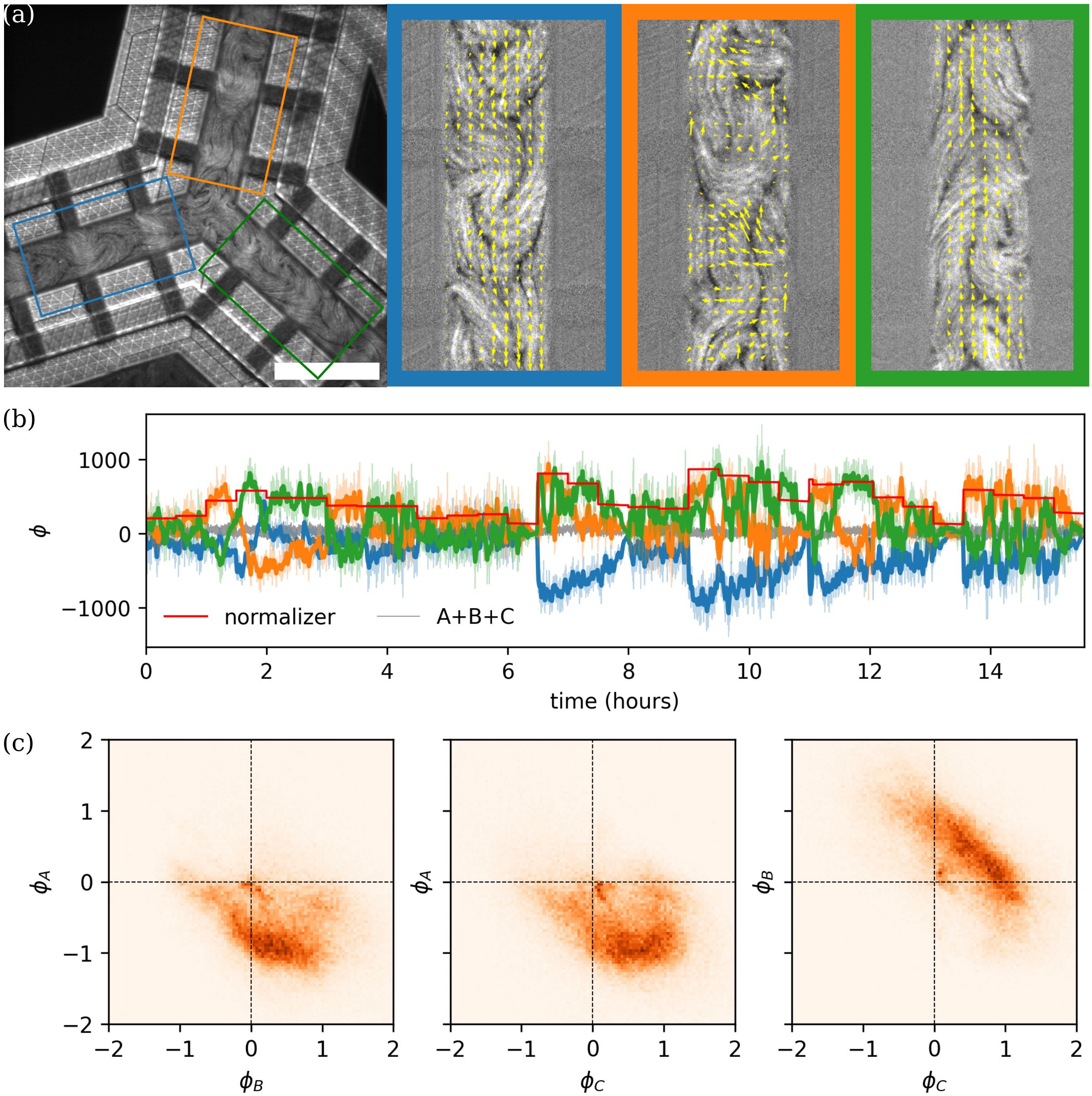

FIG. 2. **Flow rate measurements and flow rate histogram.** (a) A snapshot of microtubule-kinesin system confined in bifurcation channels. The scale bar is 200 μm. The 3 panels on the right are crops of each channel with corresponding border colors. The yellow arrows are the results from PIV analysis. (b) Flow rate time series in the 3 channels A (blue), B (orange) and C (green). The light and thin curves in the back are the real flow rates, while the strong and thick curves in the front are Gaussian-smoothed flow rates with $\sigma = 25$ s. The red curve is the "normalizer", defined as the maximum of the smoothed absoluted flow rates in A, B and C. The gray curve is the sum of the flow rates in the 3 channels, which is used to verify the continuity at the junction. The unit of flow rate is $\mu\text{m}^2/\text{s}$. Note that the direction away from the junction is defined as the positive direction. (c) The histogram of normalized flow rates. From left to right ϕ_A-ϕ_B, ϕ_A-ϕ_C and ϕ_B-ϕ_C. Note that these histograms are not independent since the 3 flow rates satisfy $\phi_A + \phi_B + \phi_C = 0$. Therefore, in the following, we only show ϕ_B-ϕ_C histogram. Down size this figure and the figures in the following. No need to show flow rate time series. Labels can be relaxed.

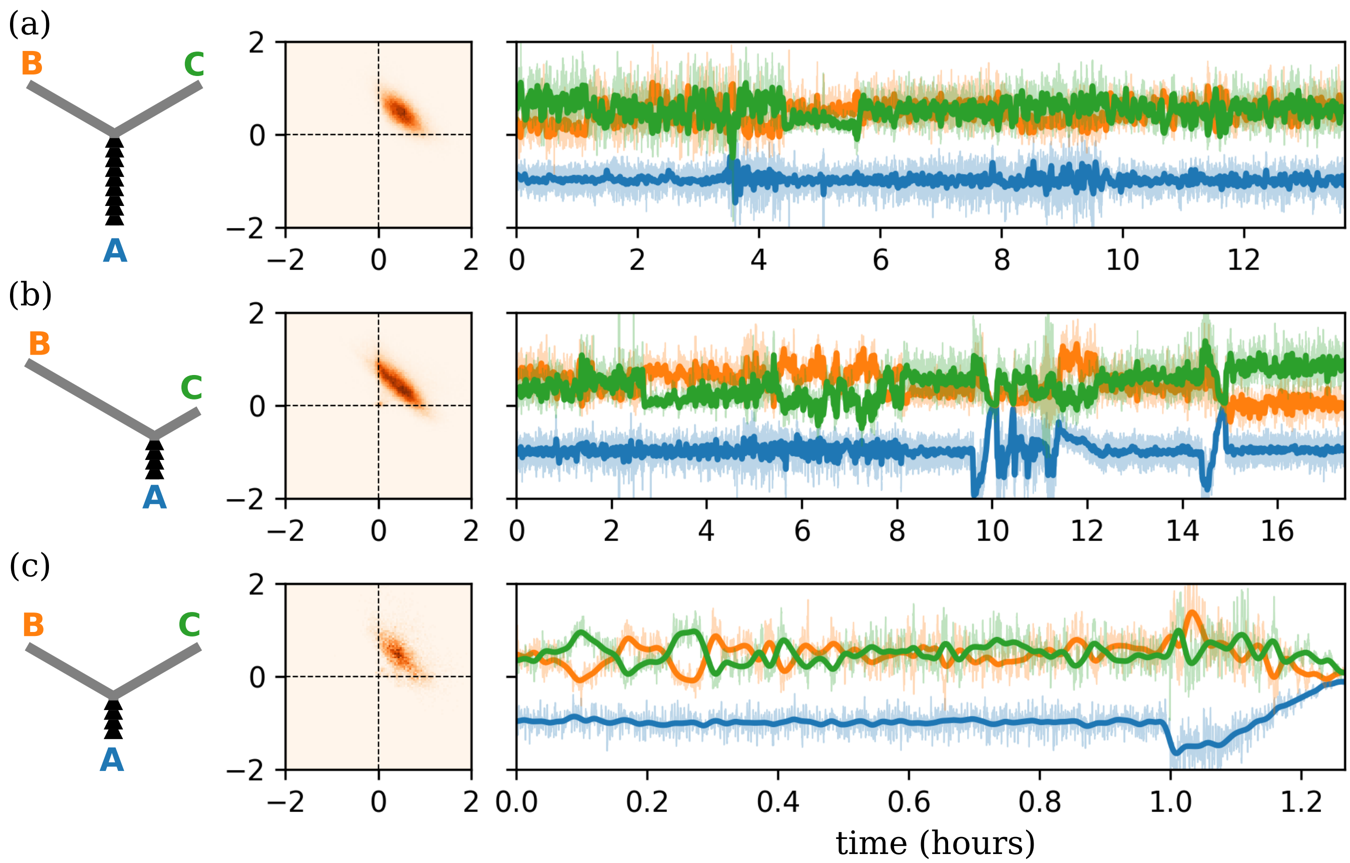

FIG. 3. **Ratchet inlet and straight outlets: histogram and time series.** (a) 9-teeth ratchet inlet with 2 equal length outlets. The flow fluctuates between polarized and non-polarized states, exploring all the possible configurations. The equal splitting state is the most probable configuration. (b) 4-teeth ratchet inlet with long and short outlets. The flow also explores all the possible configurations, but shows no preferred splitting ratio. (c) 4-teeth ratchet inlet with 2 equal length outlets. The flow fluctuates between polarized and non-polarized states, exploring all the possible configurations. The equal splitting state is the most probable configuration.

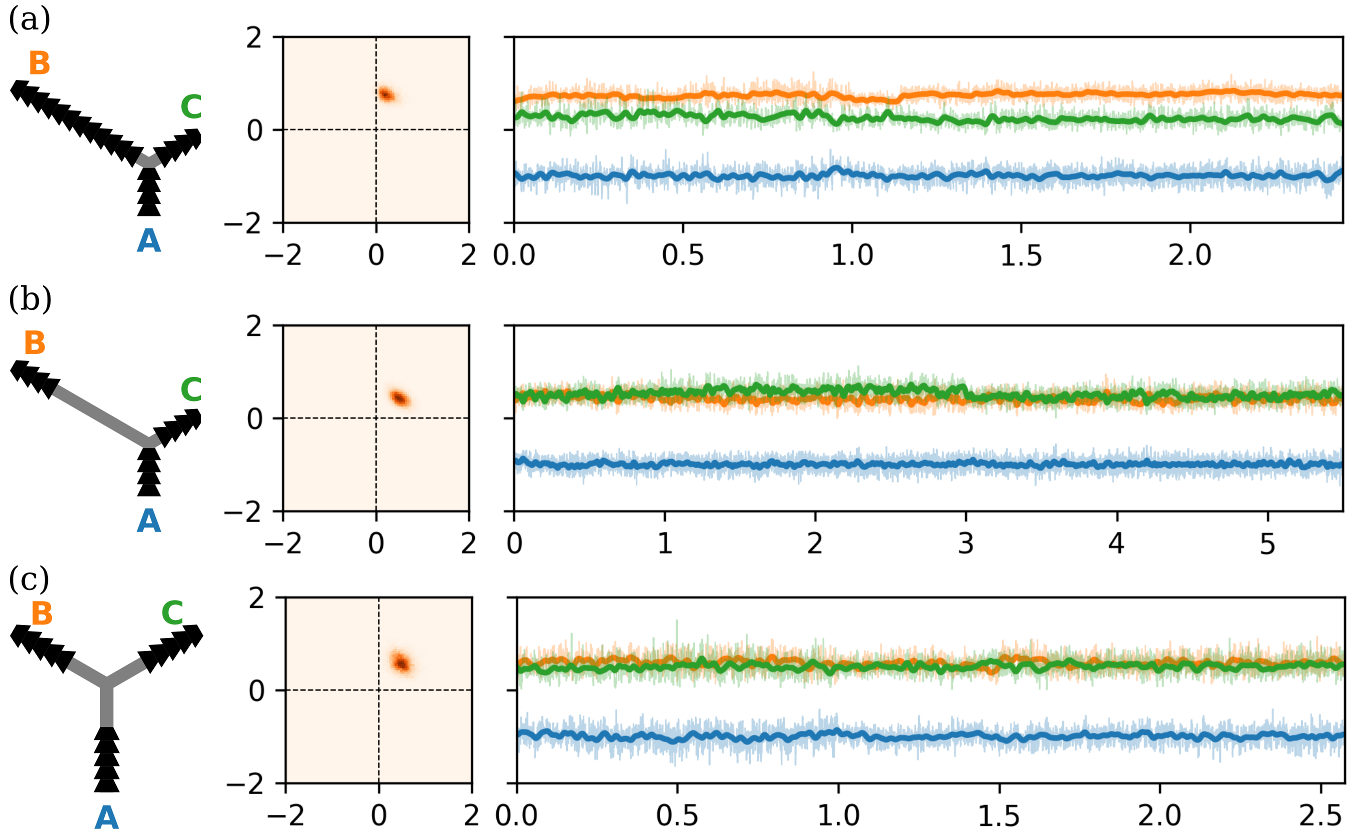

FIG. 4. **Ratchet inlet and outlets: histogram and time series.** (a) The numbers of ratchet teeth in channels A, B and C are 4, 13 and 4, respectively. Let's refer to this bifurcation channel network 4-13-4 bifurcation. In contrast to straight channels, the flows exhibit a sharp peak in the histogram, while other splitting ratios remain rarely explored. The splitting ratio is around 3:1. (b) 4-4-4 bifurcation, where channel B has an extended straight portion. The flows again exhibit a sharp peak in the histogram at a splitting ratio around 1:1. (c) 5-5-5 bifurcation, where all the channels are of the same length. The flows again exhibit a sharp peak in the histogram at a splitting ratio around 1:1.

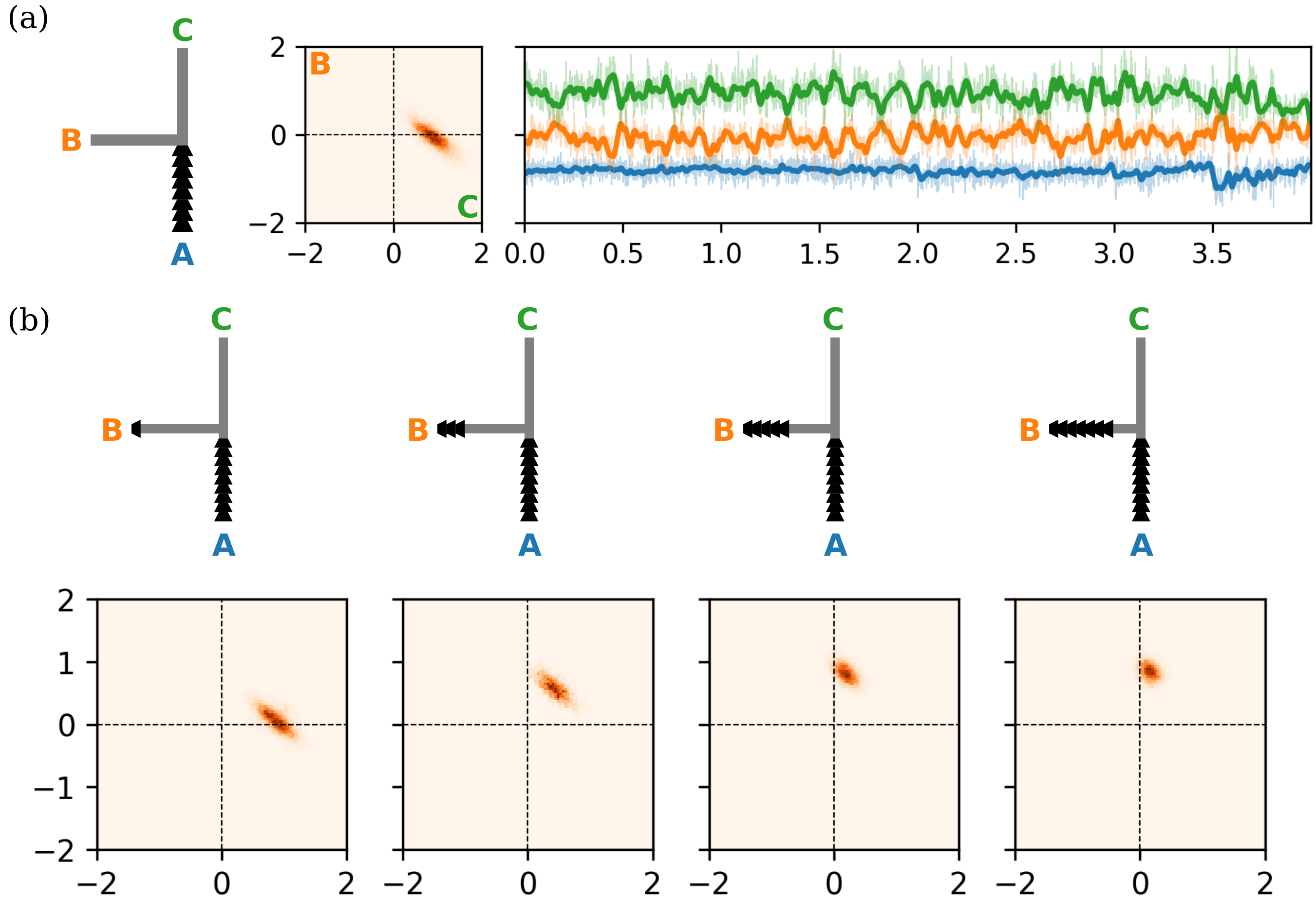

FIG. 5. **The role of turning angles.** (a) A bifurcation with a 9-teeth ratchet inlet and 2 straight outlets of the same length. The outlets have different turning angles with respect to the inlet channel A: $\angle AOB = 90°$ and $\angle AOC = 180°$. The flow rate histogram and time series suggest that the flow prefers the 180° channel C, i.e. the channel parallel to the inlet channel A, rather than channel B which requires a 90° turn. (b) Adding various numbers of ratchets to channel B to compete with the 90° turning angle. From left to right, 1, 3, 5, 7 ratchet teeth are added to the end of channel B. Below the schematics of bifurcation channels are the ϕ_B-ϕ_C flow rate histograms corresponding to the design above. As the number of ratchet teeth in channel B is increased, the splitting ratio between B and C is increase from 0 to ∞.